Mixed-Mode S-Parameter Characterisation of Differential Structures

W. Fan, A. C. W. Lu, L. L. Wai and B. K. Lok

Abstract – Combined differential-mode and common-mode (mixed-mode) scattering parameters (s-parameters) are well adapted for accurate measurements of linear networks at RF and microwave frequencies. The relationships between standard s-parameters with two-port vector network analyser (VNA) and mixed-mode s-parameters with four-port VNA are derived in this paper. A fabricated differential structure was measured with standard two-port VNA and mixed-mode four-port VNA. The correlation between standard s-parameters and mixed-mode s-parameters is presented as well.

Keywords: Mixed-mode s-parameter, Differential structure, Balance transmission line, Multi-port VNA

1 BACKGROUND

The differential structures are widely used in RF, microwave and high-speed broadband applications. The evaluation of differential structures is necessary to ensure optimal circuit and system performance. Combined differential-mode and common-mode (mixed-mode) scattering parameters (s-parameters) are well adapted to accurate measurements of linear networks at RF frequencies. However, differential structure measurements with a traditional two-port vector-network analyser (VNA) present many challenges [1-2]. The major obstacle in RF application of differential structures is that most test equipment is intended for single-ended devices. The related infrastructure is also unbalanced, such as calibration standards, transmission lines and connectors, and even industry standard reference impedance [3-4]. This paper presents the transformation between standard s-parameters and mixed-mode s-parameters. A fabricated differential structure is measured with two-port VNA and four-port mixed-mode VNA, respectively, and the correlation data is presented as well. Although the standard transformation technique could ideally be used to allow a traditional two-port VNA to carry out measurements of mixed-mode s-parameters, a mix-mode measurement system is essential to accurately characterize the effect of mode-conversion in the real differential test structures accurately [1].

2 OBJECTIVE

The main objective of this work was to build up the in-house capability in SIMTech on development of techniques and methodologies for multi-port characterization up to 20 GHz.

3 METHODOLOGY

3.1 Standard-mode and mixed-mode S-parameter of differential structure

For single-ended devices, RF voltages and currents relative to a common ground can be defined at each terminal of the device. From the voltage, current and impedance definitions, normalized power waves can be defined as stimulus and response. Stimulus power waves propagate into the device-under-test (DUT), and response power waves propagate away from it. A block diagram of a four-port device is shown in Fig. 1.

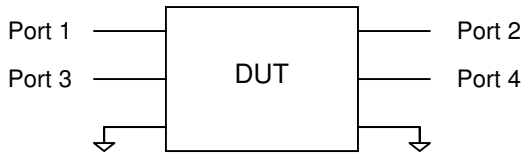

Fig. 1. Diagram of single-ended 4-port DUT.

$$\begin{bmatrix} b_1 \\ b_2 \\ b_3 \\ b_4 \end{bmatrix} = \begin{bmatrix} S_{11} & S_{12} & S_{13} & S_{14} \\ S_{21} & S_{22} & S_{23} & S_{24} \\ S_{31} & S_{32} & S_{33} & S_{34} \\ S_{41} & S_{42} & S_{43} & S_{44} \end{bmatrix} \begin{bmatrix} a_1 \\ a_2 \\ a_3 \\ a_4 \end{bmatrix} \quad (1)$$

The relationship between the power waves is shown in Eq. (1) where $B_{std} = S_{std}\, A_{std.}$ $B_{std.}$ and A_{std} represents response and stimulus waves' matrix respectively; whereas S_{std} is the standard four-port s-parameters matrix. The matrix representation is shown in (2) and (3) respectively.

$$B_{std} = \begin{bmatrix} b_1 \\ b_2 \\ b_3 \\ b_4 \end{bmatrix} \qquad A_{std} = \begin{bmatrix} a_1 \\ a_2 \\ a_3 \\ a_4 \end{bmatrix} \tag{2}$$

$$S_{std} = \begin{bmatrix} S_{11} & S_{12} & S_{13} & S_{14} \\ S_{21} & S_{22} & S_{23} & S_{24} \\ S_{31} & S_{32} & S_{33} & S_{34} \\ S_{41} & S_{42} & S_{43} & S_{44} \end{bmatrix} \tag{3}$$

For balanced devices, differential- and common-mode voltages and currents can be defined on each balanced port. Similarly differential- and common-mode impedances can also be defined. A block diagram of a two-port differential DUT is shown in Fig. 2.

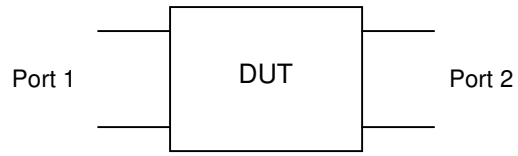

Fig. 2. Diagram of differential 2-port DUT.

A mixed-mode s-matrix in (4) can be organized such that it is similar to the single-ended s-matrix, where each column (row) represents a different stimulus (response) condition. The mode information as well as port information must be included in the mixed-mode s-matrix [3].

$$\begin{bmatrix} b_{d1} \\ b_{d2} \\ \hline b_{c1} \\ b_{c2} \end{bmatrix} = \left[\begin{array}{cc|cc} S_{d1d1} & S_{d1d2} & S_{d1c1} & S_{d1c2} \\ S_{d2d1} & S_{d2d2} & S_{d2c1} & S_{d2c2} \\ \hline S_{c1d1} & S_{c1d2} & S_{c1c1} & S_{c1c2} \\ S_{c2d1} & S_{c2d2} & S_{c2c1} & S_{c2c2} \end{array}\right] \begin{bmatrix} a_{d1} \\ a_{d2} \\ \hline a_{c1} \\ a_{c2} \end{bmatrix} \tag{4}$$

S_{didj} and S_{cicj} (*i, j=1, 2*) are the differential-mode and common-mode s-parameters respectively. S_{dicj} and S_{cidj} (*i, j=1, 2*) are the mode-conversion or cross-mode s-parameters. Differential response is represented by the parameters S_{didj} (*i, j=1, 2*) in the upper left corner of the mixed-mode s-matrix (4) due to a differential stimulus. Conversion of common-mode (differential-mode) waves into differential-mode (common-mode) waves is characterized by S_{dicj} (S_{cidj}) (*i, j=1, 2*) parameters.

3.2 Transformation between Standard-mode and mixed-mode S-parameter

The mixed-mode s-parameters in (4) can be directly related to standard four port s-parameters (3) if nodes 1 and 2 in Fig. 1 are approximated as a single differential port. Similarly nodes 3 and 4 are also grouped as another differential port [5]. The relationship between the response and stimulus of standard-mode and mixed-mode are shown in (5) and (6) respectively. a_i and b_i (*i=1 to 4*) are the waves measured at ports 1-4 in Fig. 1.

$$\begin{aligned} a_{d1} &= \frac{1}{\sqrt{2}}(a_1 - a_3) \\ a_{c1} &= \frac{1}{\sqrt{2}}(a_1 + a_3) \\ b_{d1} &= \frac{1}{\sqrt{2}}(b_1 - b_3) \\ b_{c1} &= \frac{1}{\sqrt{2}}(b_1 + b_3) \end{aligned} \tag{5}$$

$$\begin{aligned} a_{d2} &= \frac{1}{\sqrt{2}}(a_2 - a_4) \\ a_{c2} &= \frac{1}{\sqrt{2}}(a_2 + a_4) \\ b_{d2} &= \frac{1}{\sqrt{2}}(b_2 - b_4) \\ b_{c2} &= \frac{1}{\sqrt{2}}(b_2 + b_4) \end{aligned} \tag{6}$$

The transformation matrix in (12) between standard s-parameters and mixed-mode s-parameters can be derived from the following equations: mixed-mode incident waves A_{mm} in (7); mixed-mode response waves B_{mm} in (8); mixed-mode s-parameters matrix S_{mm} in (11); standard four port s-parameters matrix S_{std} in (3); and the conversion matrix M in (9) and M^{-1} in (10).

$$\begin{aligned} A_{mm} &= MA_{std} \\ &= \begin{bmatrix} a_{d1} \\ a_{d2} \\ a_{c1} \\ a_{c2} \end{bmatrix} = \frac{1}{\sqrt{2}} \begin{bmatrix} 1 & 0 & -1 & 0 \\ 0 & 1 & 0 & -1 \\ 1 & 0 & 1 & 0 \\ 0 & 1 & 0 & 1 \end{bmatrix} \begin{bmatrix} a_1 \\ a_2 \\ a_3 \\ a_4 \end{bmatrix} \end{aligned} \tag{7}$$

$$\begin{aligned} B_{mm} &= MB_{std} \\ &= \begin{bmatrix} b_{d1} \\ b_{d2} \\ b_{c1} \\ b_{c2} \end{bmatrix} = \frac{1}{\sqrt{2}} \begin{bmatrix} 1 & 0 & -1 & 0 \\ 0 & 1 & 0 & -1 \\ 1 & 0 & 1 & 0 \\ 0 & 1 & 0 & 1 \end{bmatrix} \begin{bmatrix} b_1 \\ b_2 \\ b_3 \\ b_4 \end{bmatrix} \end{aligned} \tag{8}$$

$$M = \frac{1}{\sqrt{2}} \begin{bmatrix} 1 & 0 & -1 & 0 \\ 0 & 1 & 0 & -1 \\ 1 & 0 & 1 & 0 \\ 0 & 1 & 0 & 1 \end{bmatrix} \tag{9}$$

$$M^{-1} = \frac{M^*}{|M|} = \frac{1}{\sqrt{2}} \begin{bmatrix} 1 & 0 & 1 & 0 \\ 0 & 1 & 0 & 1 \\ -1 & 0 & 1 & 0 \\ 0 & -1 & 0 & 1 \end{bmatrix} \tag{10}$$

$$B_{mm} = S_{mm} A_{mm} = \begin{bmatrix} b_{d1} \\ b_{d2} \\ b_{c1} \\ b_{c2} \end{bmatrix} = \begin{bmatrix} S_{d1d1} & S_{d1d2} & S_{d1c1} & S_{d1c2} \\ S_{d2d1} & S_{d2d2} & S_{d2c1} & S_{d2c2} \\ S_{c1d1} & S_{c1d2} & S_{c1c1} & S_{c1c2} \\ S_{c2d1} & S_{c2d2} & S_{c2c1} & S_{c2c2} \end{bmatrix} \begin{bmatrix} a_{d1} \\ a_{d2} \\ a_{c1} \\ a_{c2} \end{bmatrix} \quad (11)$$

$$S_{mm} = M S_{std} M^{-1} = \begin{bmatrix} \begin{bmatrix} S_{d1d1} & S_{d1d2} \\ S_{d2d1} & S_{d2d2} \end{bmatrix} & \begin{bmatrix} S_{d1c1} & S_{d1c2} \\ S_{d2c1} & S_{d2c2} \end{bmatrix} \\ \begin{bmatrix} S_{c1d1} & S_{c1d2} \\ S_{c2d1} & S_{c2d2} \end{bmatrix} & \begin{bmatrix} S_{c1c1} & S_{c1c2} \\ S_{c2c1} & S_{c2c2} \end{bmatrix} \end{bmatrix}$$

$$= \frac{1}{2} \begin{bmatrix} \begin{bmatrix} S_{11} - S_{13} - S_{31} + S_{33} & S_{12} - S_{14} - S_{32} + S_{34} \\ S_{21} - S_{23} - S_{41} + S_{43} & S_{22} - S_{24} - S_{42} + S_{44} \end{bmatrix} & \begin{bmatrix} S_{11} + S_{13} - S_{31} - S_{33} & S_{12} + S_{14} - S_{32} - S_{34} \\ S_{21} + S_{23} - S_{41} - S_{43} & S_{22} + S_{24} - S_{42} - S_{44} \end{bmatrix} \\ \begin{bmatrix} S_{11} - S_{13} + S_{31} - S_{33} & S_{12} - S_{14} + S_{32} - S_{34} \\ S_{21} - S_{23} + S_{41} - S_{43} & S_{22} - S_{24} + S_{42} - S_{44} \end{bmatrix} & \begin{bmatrix} S_{11} + S_{13} + S_{31} + S_{33} & S_{12} + S_{14} + S_{32} + S_{34} \\ S_{21} + S_{23} + S_{41} + S_{43} & S_{22} + S_{24} + S_{42} + S_{44} \end{bmatrix} \end{bmatrix} \quad (12)$$

4 RESULTS & DISCUSSION

The test vehicle is a 4-layer FR4 substrate with a coupled differential structure design. The cross section and fabricated test board are shown in Fig. 3 and 4 respectively. The cross section illustrates a microstrip topology and the test vehicle parameters are shown in Table 1. The test structure was designed as a tightly-coupled microstrip differential structure and its differential impedance is 100 Ohm. The SMA connectors were used for the VNA connection.

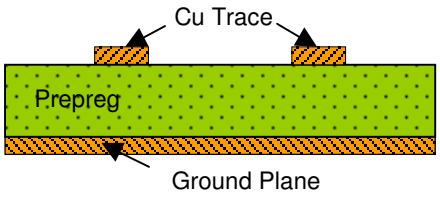

Fig. 3. Cross-section of test board.

Fig. 4. Fabricated test board.

Table 1. Test board parameters.

Copper (Cu)	Thickness (µm)	42.5
	Line Width (µm)	290
	Spacing (µm)	510
Prepreg	Thickness (µm)	190
	Dielectric Constant, εr	4.0
	Loss Tangent δ	0.02

The set up of single-ended two-port VNA measurement is shown in Fig. 5(a). During the two-port VNA measurement, any two ports on the DUT is connected to two-port VNA respectively, and the two remaining ports were terminated with 50 Ohm. All combinations of four individual ports are measured to get standard s-parameters matrix, i.e. P1&P2, P1&P3, P1&P4, P2&P3, P2&P4 and P3&P4. These two-port measurement results can be used to form standard four-port s-parameters matrix S_{std} in (3). Standard s-parameters matrix S_{std} will be converted into mixed-mode s-parameters matrix S_{mm} in (12). The setup of differential-ended four-port VNA measurement is shown in Fig. 5(b). All four ports on the DUT are connected to mixed-mode four-port VNA. The calibration method of short-open-load-through (SOLT) is used for both two-port and four-port VNA.

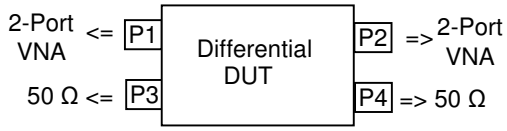

(a) For single-ended 2-port VNA.

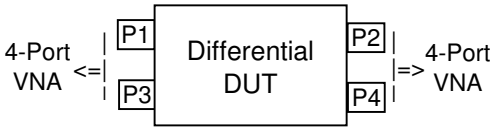

(b) For differential-ended 4-port VNA.

Fig. 5. Setup of s-parameters measurement .

In Figs. 6 to 14, the curves denoted as “Standard” represent the mixed-mode s-parameters converted from two-port VNA measurements, and the curves denoted as “Mixed” represent the mixed-mode s-parameters measured with

mixed-mode four-port VNA. In Fig. 6, the insertion loss Sd1d2 of differential response and differential stimulus has a very good agreement between “Standard” and “Mixed”. The curve denoted as “Single-Ended S12” is shown as a reference for the insertion loss between single-ended port 1 and single-ended port 2.

The insertion (return) loss of response and stimulus with same mode has a very good correlation between “Standard” and “Mixed” mode s-parameters in Fig. 7 to 10. For the response and stimulus with different mode, there is a slight variation between “Standard” and “Mixed” mode s-parameters for both insertion and return loss shown in Fig. 11 to 14. It can be seen that the mode conversion method between standard and mixed-mode s-parameters can be used to characterize the differential structures for the users who only have traditional two-port VNA.

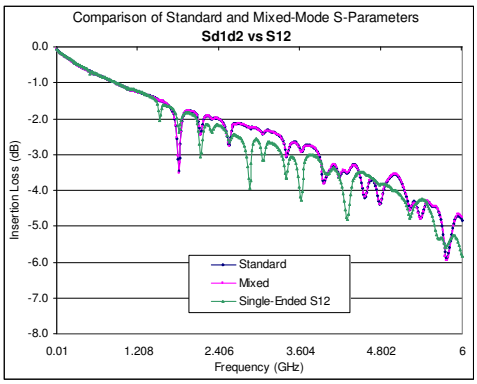

Fig. 6. Insertion loss in single-ended and differential-ended structure.

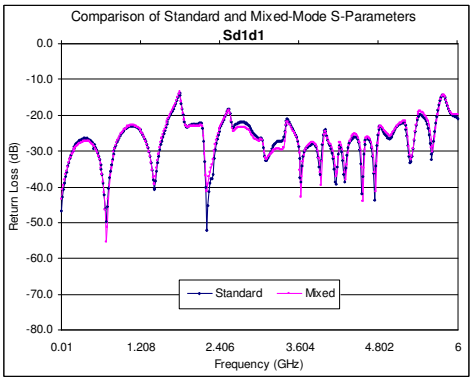

Fig. 7. Return loss in differential-mode of response and stimulus.

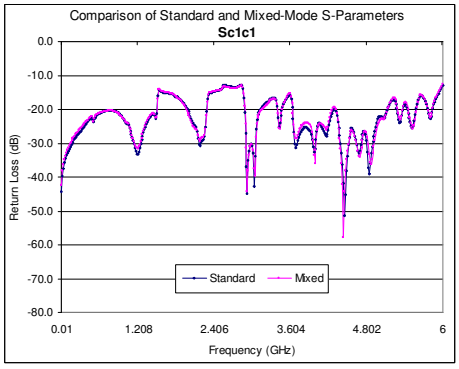

Fig. 8. Return loss in common-mode of response and stimulus.

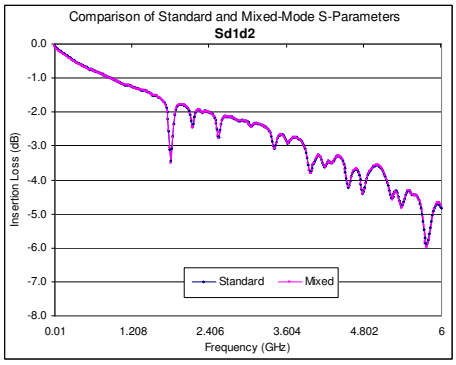

Fig. 9. Insertion loss in differential-mode of response and stimulus.

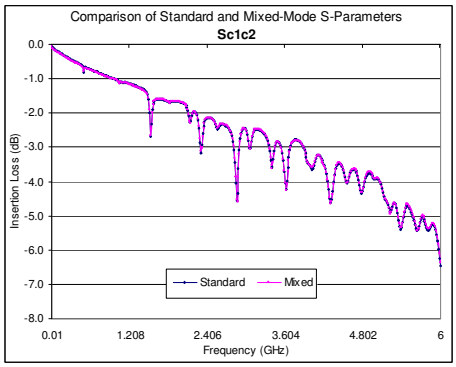

Fig. 10. Insertion loss in common-mode of response and stimulus.

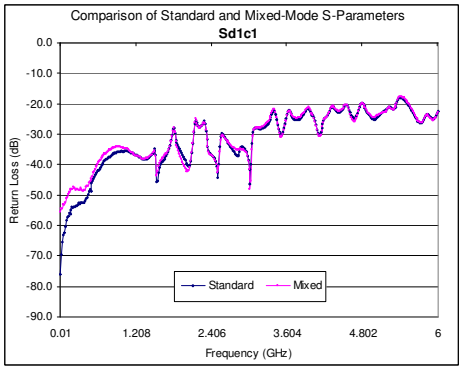

Fig. 11. Differential-mode response and common-mode stimulus.

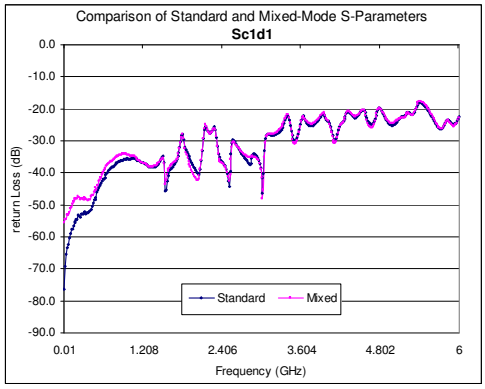

Fig. 12. Common-mode response and differential-mode stimulus.

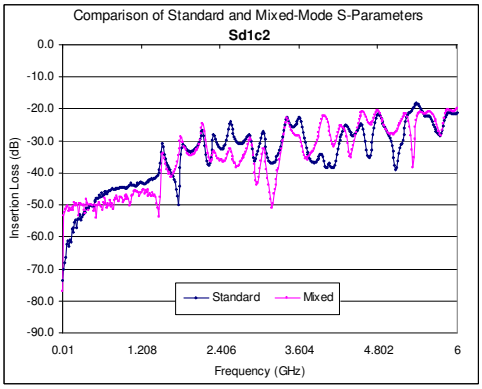

Fig. 13. Differential-mode response and common-mode stimulus.

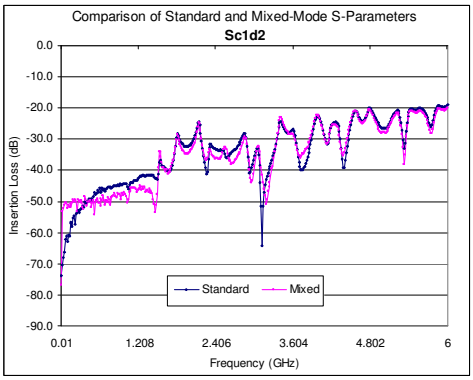

Fig. 14. Common-mode response and differential-mode stimulus.

5 CONCLUSION

Mode transformation between standard s-parameters and mixed-mode s-parameters has been presented in this paper. Characterization of fabricated differential structure has demonstrated that there is a close correlation between the mixed-mode s-parameters converted from two-port VNA and mixed-mode four-port VNA measurements. The mixed-mode s-parameters derived from the two methods have good agreement for the stimulus and response with the same mode (common or differential), and a small variation for the stimulus and response with different modes (common/differential, differential/common). In order to predict the behaviour of the mixed-mode s-parameters using a traditional two-port VNA, the mode transformation technique can be applied, however, a mixed-mode four-port VNA system is still required to accurately measure the impact of mode conversion in real integrated differential test structures.

6 INDUSTRIAL SIGNIFICANCE

PCB manufacturers, test service providers and communication transceiver manufacturers will benefit from the techniques and methodologies for multi-port characterization developed in this work.

REFERENCES

[1] D.E. Bockelman and W.R. Eisenstadt, “Pure-Mode Network Analyzer for On-Wafer Measurements of Mixed-Mode S-Parameters of Differential Circuits,” *IEEE Trans. Microwave Theory Tech.*, Vol. 43, pp. 1071-1077, (1997).

[2] D.E. Bockelman and W.R. Eisenstadt, “Combined differential and common-mode scattering parameters: Theory and simulation,” *IEEE Trans. Microwave Theory Tech.*, Vol. 43, pp. 1530-1539, (1995).

[3] Application Notes: *Balanced Device Characterization*, Agilent Technologies, (2002).

[4] Application Note 1373-1: *An Introduction to Multiport and Balanced Device Measurements*, Agilent Technologies,(2002).

[5] K. Kurokawa, “Power Waves and the Scattering Matrix”, *IEEE Trans. Microwave Theory Tech.*, Vol. 13, pp. 194-202, (1965).